Application of Microplasma for NO_X Removal

Kazuo Shimizu, *Member, IEEE*, Takeki Sugiyama, Manisha Nishamani L. S., and Masaki Kanamori

***Abstract*—In this paper, microplasma is investigated, which occurs between the narrow gap of the electrodes covered with dielectric materials. The discharge gap is set on the order of micrometers by changing a spacer from 0 to 100 μm. In this paper, the characteristics of microplasma, such as discharge voltages, discharge currents, and discharge power that is obtained with the help of Lissajous figures, and the relationships between these electric characteristics are presented. The characteristics of ozone generation by a microplasma electrode are investigated. Treatment by microplasma for the simulated exhaust gas, which contains NO_x and C_3H_8 as a role of HC and CO, is estimated experimentally. In the absence of O_2, the exhaust gas is decomposed by nitrogen atomic species in particular. In the presence of O_2, it is decomposed by nitrogen atomic species and oxidized by ozone. By-product analysis of treated gases is carried out by Fourier transform infrared spectroscopy and gas chromatography–mass spectrometry. When HC, NO_x, and N_2 are included in the simulated exhaust gas, HCN, N_2O, and CH_4 are confirmed as by-products of the microplasma treatment.**

***Index Terms*—Air pollution control, exhaust gas, microplasma, NO_x, ozone.**

I. Introduction

NONTHERMAL plasma is widely used for environmental protection and plasma-enhanced chemical synthesis or reaction, particularly ozone generation [1]–[4] and polluted gas control such as dissociations of NO_x and HC with a dielectric barrier discharge [5]–[12] and a pulsed corona [13]–[15].

Microplasma could be generated at lower discharge voltages than those discharge methods because of its narrow gaps. Therefore, the size of the power source of microplasma could be smaller than that of a corona discharge and an atmospheric glow discharge.

Paper MSDAD-09-03, presented at the 2007 Industry Applications Society Annual Meeting, New Orleans, LA, September 23–27, and approved for publication in the IEEE Transactions on Industry Applications by the Electrostatic Processes Committee of the IEEE Industry Applications Society. Manuscript submitted for review December 15, 2007 and released for publication February 9, 2009. First published May 19, 2009; current version published July 17, 2009. This work was supported in part by the Ministry of Education, Science, Sports and Culture under Grant-in-Aid for Young Scientists (A)17681007, 2007, and in part by the Japan Science and Technology Agency, Grant Program of Research for Promoting Technological Seed and Potentiality Verification Stage.

K. Shimizu is with the Innovation and Joint Research Center, Shizuoka University, Hamamatsu 432-8561, Japan (e-mail: shimizu@cjr.shizuoka.ac.jp).

T. Sugiyama is with Shizuoka Gas Company, Ltd., Shizuoka 420-0913, Japan (e-mail: takeki.s@hotmail.co.jp).

M. Nishamani L. S. is with the Royal Institute of Technology, 100 44 Stockholm, Sweden (e-mail: manisha.siri@gmail.com).

M. Kanamori was with the Innovation and Joint Research Center, Shizuoka University, Hamamatsu 432-8561, Japan. He is now with the Toshiba Carrier Corporation, Tokyo 108-0074, Japan (e-mail: goldmori@hotmail.com).

Color versions of one or more of the figures in this paper are available online at http://ieeexplore.ieee.org.

Digital Object Identifier 10.1109/TIA.2009.2023494

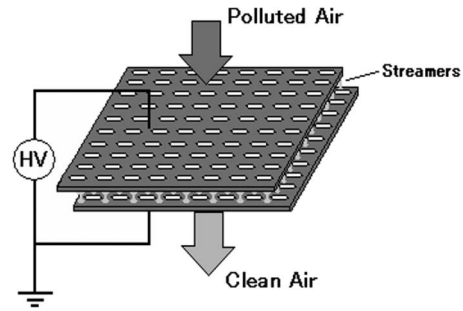

Fig. 1. Schematic image of microplasma electrodes. The pressure loss between the electrodes is very small.

This point would be significant for indoor-air or exhaust-gas treatment, particularly for small cars or motorcycles. We have investigated the feasibility of microplasma for removing the simulated exhaust gas of gasoline engines. Microplasma could be generated at a discharge gap of less than 100 μm, particularly 10 μm with only around 1 kV.

Recently, the characteristics of microplasma have been investigated [16]. There are few applications for environmental protection such as formaldehyde removal of indoor air [17], [18].

II. About Microplasma

Fig. 1 shows a schematic image of the electrodes used in the experiments. It is a stainless steel covered with dielectric barrier materials in both faces and is 120 cm^2 in area. The thickness of the dielectric material is 100 μm (Fig. 2). There are many holes in the electrode with $\varnothing$ 1.5 mm that results in an aperture ratio of 25%.

The gas is flowed through the holes and reacted with electrons between the electrodes, which are supplied with a self-made high-voltage ac power. The pressure loss is about 30-mmH_2O in a gas flow rate of 8.5 L/min. The pressure loss is very small, and this reactor could be applied to exhaust-gas treatments with large gas flows.

In this experiment, the discharge gap between the electrodes is set to less than 100 μm to realize the minimum sparking voltage at atmospheric pressure based on Pachen's law. Table I shows the minimum sparking voltage and the minimum gaps for air, nitrogen, and oxygen.

Fig. 3 shows a schematic image of the removal process of microplasma between the electrodes. The simulated exhaust gas contains NO_x, and HC and CO could be decomposed by atomic oxygen and the nitrogen species generated between the electrodes.

Due to the assumed value of the dielectric constant of the dielectric material $\varepsilon_{r1} = 10^4$ and according to

$$\boldsymbol{D} = \varepsilon_1 \boldsymbol{E}_1 = \varepsilon_2 \boldsymbol{E}_2 \quad (1)$$

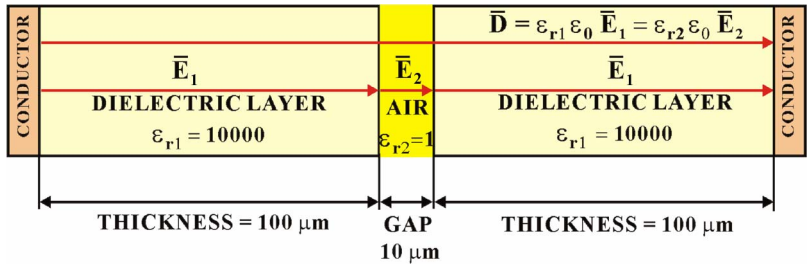

Fig. 2. Electric field inside the capacitor formed by a pair of electrodes consisted in two dielectric layers and the air gap. Due to the high dielectric constant of the dielectric layer $\varepsilon_{r1} = 10^4$, a high-intensity electric field in the air gap $E_2 = 10^7 - 10^8$ V/m is obtained.

TABLE I
MINIMUM SPARKING VOLTAGE AND DISCHARGE GAP FOR VARIOUS GASES

Gas	minimum sparking voltage [V]	minimum gap [um]
Air	330	7.5
Oxygen	450	9.2
Nitrogen	275	9.9

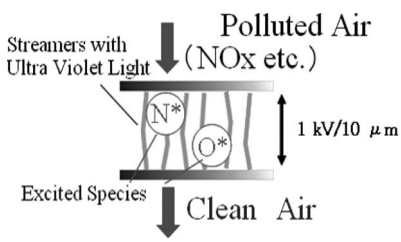

Fig. 3. Schematic image of the removal process of microplasma between the electrodes.

where D is the electric displacement field, E_1 and E_2 are the intensities of the electric field in the dielectric layer and in the air gap, respectively, and $\varepsilon_1 = \varepsilon_{r1}\varepsilon_0$ and $\varepsilon_2 = \varepsilon_{r2}\varepsilon_0$ are the permittivities, respectively, of the dielectric layer and of the air, where ε_0 is the vacuum permittivity, it results in

$$\boldsymbol{E}_2 = \frac{\varepsilon_{r1}\varepsilon_0}{\varepsilon_{r2}\varepsilon_0}\boldsymbol{E}_1 = 10^4\boldsymbol{E}_1. \quad (2)$$

At a gap between the electrodes of 10 μm and at a thickness of the dielectric barrier of 100 μm, and according to (2), a high electrical field ($E_2 = 10^7 - 10^8$ V/m) is obtained, which assures the formation of nonthermal plasma. High-energy electrons and active species are generated in such a microplasma, which is activated by high electrical field.

III. EXPERIMENTAL SETUP

A. Analysis of Gas Composition

Fig. 4 shows the experimental setup. The gas mixture is produced by using gas cylinders of N_2, NO, O_2, and C_3H_8 in order to simulate the exhaust gases from the gasoline engines at high-load conditions. Concentrations of NO_x and O_3 are measured by a chemiluminescence NO_x analyzer (Shimadzu, NOA-7000) and an ultraviolet-absorption-type ozone monitor (Ebara, EG-2001B). Concentrations of CO and HC are also measured by a CO/HC analyzer with nondispersive infrared analyzer (Horiba, MEXA-324G).

The by-products, such as HC, NO_x, CO, and CO_2, generated by a microplasma are analyzed by Fourier transform infrared spectroscopy (FTIR; Shimadzu, IRPrestige-21) and gas chromatography–mass spectrometry (Agilent, 5972 and 5890).

B. Power Source for a Microplasma

A self-made high-frequency (15–20 kHz) power source is assembled to generate a high-voltage range of around 1 kV. Due to the relatively low voltages and very small gaps necessary for generating microplasma, only a downsized power supply is needed. The high voltage supplied to the electrode and its corresponding discharge currents are measured by a high-voltage divider (Tektronix, P6015A), an ac current probe (Tektronix, P6022), and a digital oscilloscope (Tektronix, TDS 2014). Discharge power is estimated by using a Lissajous figure.

IV. CHARACTERISTICS OF MICROPLASMA

A. Discharge Voltage of Microplasma

Fig. 5 shows sample waveforms of microplasma discharge voltage and discharge current. The applied voltage is a high-frequency ac. Fig. 5 shows the discharge voltage of 1.2 kV, which is applied to the microplasma electrode, and the corresponding discharge current of 40 mA, which contains capacitive currents. The spike currents that appeared due to the microdischarges are convoluted on the current waveform and were confirmed at the steepest slopes of the discharge voltage.

Discharge power is estimated by using a Lissajous figure, as shown in Fig. 6, and by measuring the capacitance charge, which is connected between the electrode and ground.

B. Discharge Power of Microplasma

Fig. 7 shows the characteristics of the discharge power and the discharge voltage of microplasma in air. In order to set the discharge gaps, a spacer is used. In this figure, a discharge gap of 0 μm stands for the electrodes put together without any spacer. In this case, microplasma could be generated on each surface of the electrode, particularly at the circumference of the edge of each hole.

Microplasma could be generated on each surface of the electrode, particularly at the circumference of the edge of each hole. The discharge form of a microplasma electrode could be a combination of a surface discharge and a barrier discharge. Due to this reason, the corona onset voltages for 10- and 0-μm gaps

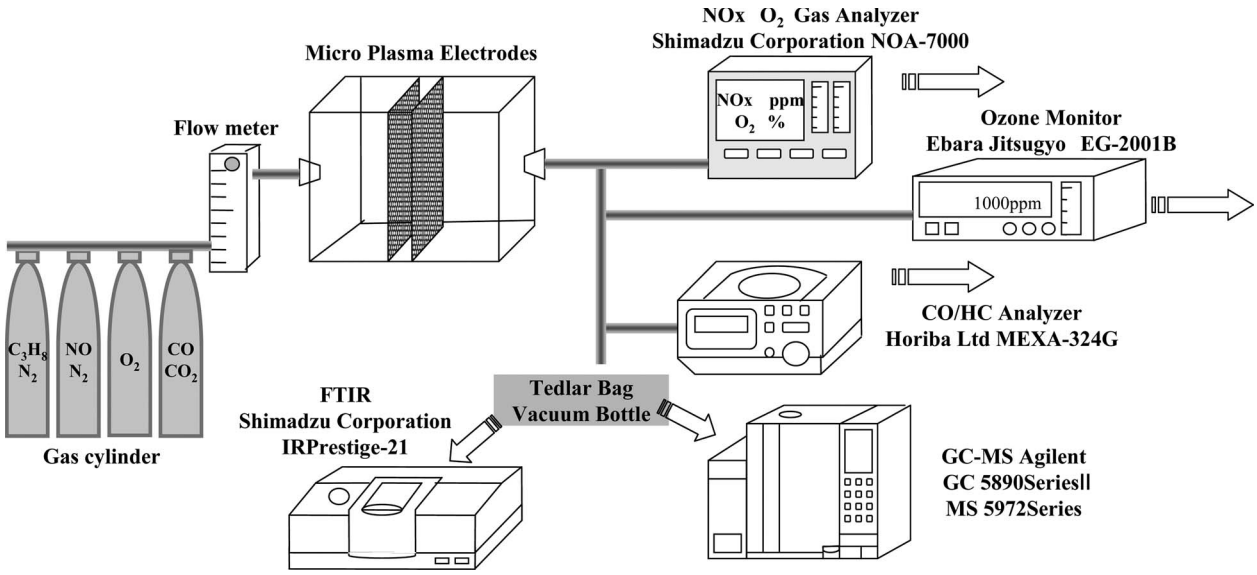

Fig. 4. Experimental setup including electrical measurements and analysis of gas composition.

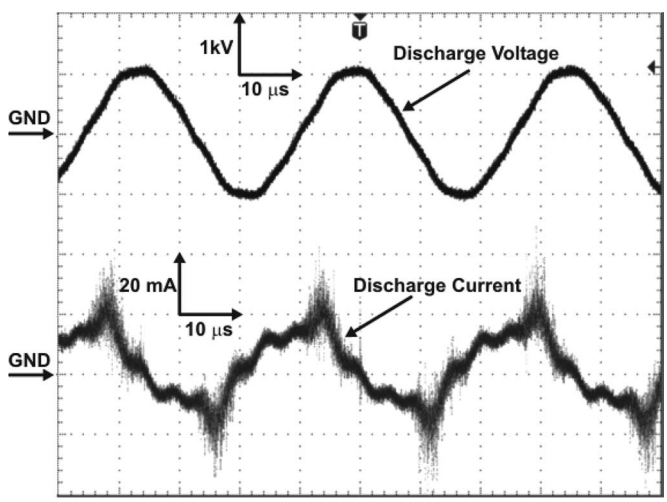

Fig. 5. Sample waveform of a discharge voltage and a discharge current.

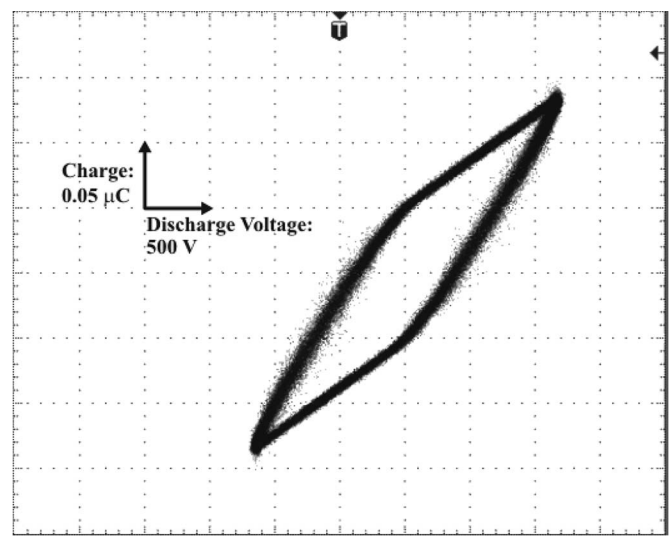

Fig. 6. Example of a Lissajous figure.

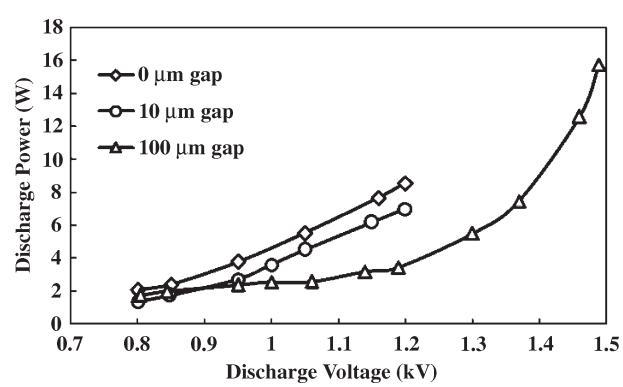

Fig. 7. Characteristics of the discharge voltage versus the discharge power at various discharge gaps.

tend to be similar. The characteristics of the discharge power also tend to be similar for the discharge gaps of 0 and 10 μm.

The sparking voltage becomes lower when the discharge gap is smaller. For example, at a discharge gap of 10 μm, discharge occurs at 0.8 kV; on the contrary, in the case of 100 μm, it occurs at 1.2 kV.

When the discharge starts, the area of the discharge was only a part of the electrode. As the discharge voltage is raised, the area spreads. Therefore, the discharge power is small when the discharge starts. With smaller discharge gap, microplasma could be generated with smaller discharge power.

V. Gas-Removal Experiment

A. NO_x Removal

Treatment of air pollutants is one of the important issues regarding global environmental protection. In this paper, NO_x, which is contained in the exhaust gas, is the target to control for one example of the treatment of microplasma.

Fig. 8 shows the NO_x removal process for the gas composition containing 100-ppm NO, 0-ppm C_3H_8, and N_2 balance and for the gas composition containing 100-ppm NO, 500-ppm C_3H_8, and N_2 balance (Table II). The objective of the

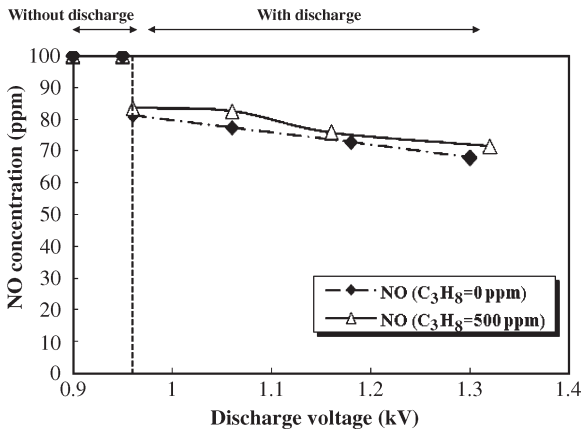

Fig. 8. Removal of NO by microplasma at a gas flow rate of 5 L/min.

TABLE II
GAS COMPOSITION OF FIG. 8

Experimental conditions	NO (ppm)	C_3H_8 (ppm)	N_2
<1> ◆	100	0	Balance
<2> △	100	500	Balance

experiments was to analyze the NO_x removal process in the presence and in the absence of C_3H_8.

The experiments were carried out at a gas flow rate of 5 L/min, a discharge gap of 10 μm, and a temperature of the gas of 25 °C.

The gas composition without C_3H_8 was treated by a microplasma. As the discharge voltage increases, the NO_x concentration decreases from 80 ppm at the beginning of the discharge process, corresponding to a discharge voltage of 0.96 kV, to 72 ppm, corresponding to a discharge voltage of 1.3 kV. NO could be chemically reduced to N_2 by atomic nitrogen species, produced by electron impact of N_2 [8]

$$e + N_2 \rightarrow e + N(^4S) + N(^4S) \tag{3}$$

$$N(^4S) + NO \rightarrow N_2 + O. \tag{4}$$

$N(^4S)$ is a ground-state nitrogen atom. The electron-impact dissociation of NO is few because the concentration of N_2 is much higher than that of NO, and most of the high-energy electrons react with N_2.

With the increase of the discharge voltage, the concentration of NO_x in the gas composition with C_3H_8 treated by a microplasma decreases from an initial concentration of 82 ppm corresponding to a discharge voltage of 0.96 kV to 78 ppm corresponding to a discharge voltage of 1.33 kV. C_3H_8 does not play a role in the dissociation of NO, since the effect of atomic nitrogen species is much larger. In this experiment, NO concentration is almost equal to NO_x concentration.

Fig. 9 shows the removal of NO_x by a microplasma at a discharge gap of 10 μm at 25 °C. The gas composition was 100-ppm NO, 5% O_2, and N_2 balance, and it was treated by a microplasma at a gas flow rate of 5 L/min.

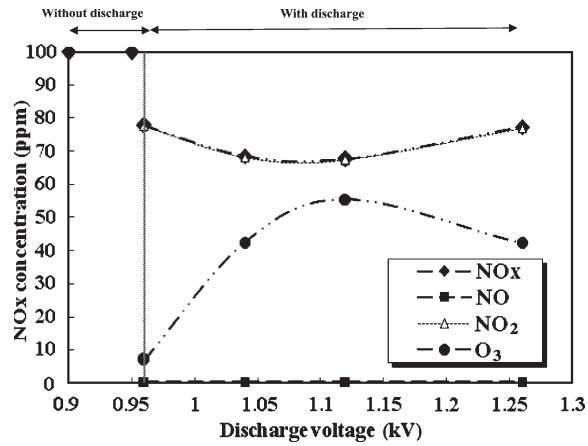

Fig. 9. Removal of NO by microplasma at a gas flow of 5 L/min. Gas composition: 100-ppm NO, 5% O_2, and N_2 balance.

With small amounts of O_2, NO could chemically be oxidized to NO_2 by O_3, which is produced by electron impact of O_2 [8]

$$e + O_2 \rightarrow e + O(^3P) + O(^3P) \tag{5}$$

$$O(^3P) + O_2 + M \rightarrow O_3 + M \tag{6}$$

$$O_3 + NO \rightarrow NO_2 + O_2 \tag{7}$$

$$NO_2 + O_3 \rightarrow NO_3 + O_2. \tag{8}$$

$O(^3P)$ is a ground-state oxygen atom, and M is either N_2 or O_2. Microplasma could be generated at a discharge voltage of about 1 kV. At a discharge voltage of 0.96 kV, the concentration of NO_x was decreased to 78 from 100 ppm. The removed quantity of NO_x increased proportionally to the discharge voltages, and the quantity of ozone increases. It has a certain peak at a discharge voltage of about 1.1 kV. This could be explained by the reaction of ozone with NO and also with NO_2 according to (7) and (8) [19]. When the discharge voltage exceeds 1.1 kV, the concentration of NO_x increases, and the quantity of ozone decreases. By increasing the discharge voltage, more atomic nitrogen species are produced, which reacts with ozone, resulting with a newly formed NO_x. NO_x is generated by the following processes [1], [8]: (5), (6), (7), and

$$O_3 + N(^4S) \rightarrow NO + O_2. \tag{9}$$

Fig. 10 shows the removal of NO_x by a microplasma at a discharge gap of 10 μm at 25 °C. The gas composition was 100-ppm NO, 5% O_2, 500-ppm C_3H_8, and N_2 balance.

With small amounts of C_3H_8, the concentration of NO_x is increased by a microplasma, and the oxidation of NO to NO_2 decreased. Almost no O_3 could be detected in this experimental condition. Most of the generated O_3 is reacted to other materials such as NO, C_3H_8, and, in particular, nitrogen atoms to be NO that is already shown in (9).

B. By-Product Analysis With FTIR

By-products must be found after the treatment of microplasma, particularly gas-phase reactions in air or exhaust gas containing various pollutants such as hydrocarbons, which generate hazardous pollutants again.

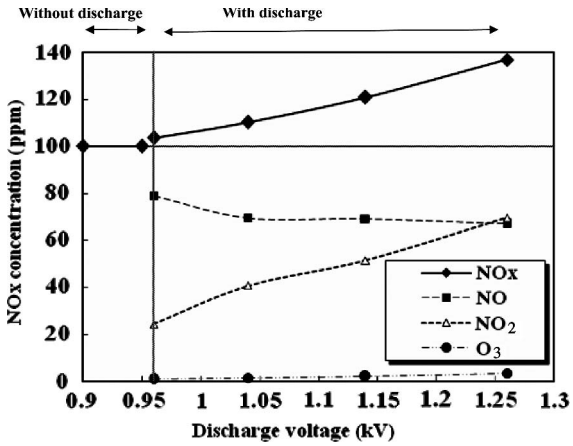

Fig. 10. Removal of NO by microplasma at a gas flow rate of 5 L/min. Gas composition: 100-ppm NO, 5% O_2, 500-ppm C_3H_8, and N_2 balance.

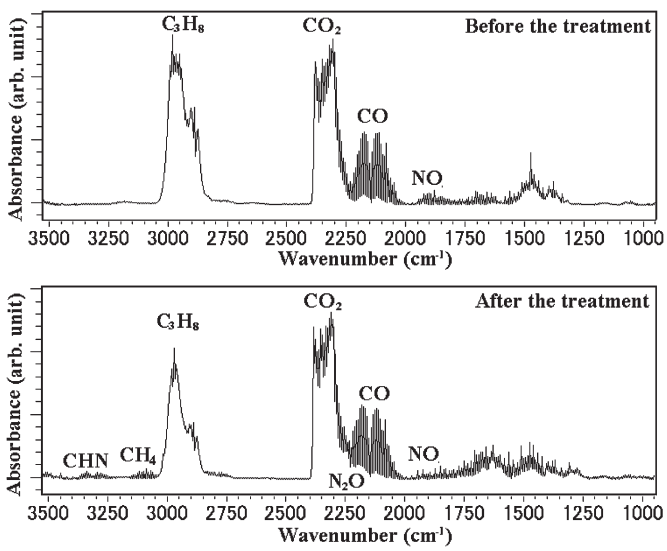

Fig. 11. By-product analysis obtained by FTIR in the absence of O_2. Gas composition: 4.02% CO, 3510-ppm C_3H_8, 1215-ppm NO, 12.02% CO_2, and N_2 balance. Discharge voltage: 1.3 kV. Discharge gap: 10 μm. Gas flow rate: 0.5 L/min.

In the case of treating NO_x with ethylene and oxygen as a simulated gas, acetaldehydes and acetic acids are found as by-products after the plasma treatment [20]. Methanol is a by-product material as a result of the conversion of methane [21], [22].

In this experiment, an FTIR and a 10-m gas cell were used to identify the final by-products of treating the simulated exhaust gases by a microplasma at a discharge gap of 10 μm. The gas cylinder adjusted the simulated gas composition of 4.02% CO, 3510-ppm C_3H_8, 1215-ppm NO, 12.02% CO_2, and N_2 balance at a gas flow rate of 0.5 L/min to increase the gas retention time between the electrodes.

Fig. 11 shows the spectra of by-product analysis obtained by FTIR in the absence of O_2. The experimental conditions of Fig. 10 are at a discharge voltage of 1.3 kV and a discharge gap of 10 μm. The upper figure shows the spectrum of before treatment with microplasma, and the lower figure shows that of after the treatment. Table III shows the changes of the concentration of simulated gases by a microplasma in the absence of O_2. The concentration of NO_x is measured by a NO_x analyzer. The concentrations of C_3H_8 and CO are cross-checked by using an FTIR analyzer and a CO/HC analyzer.

TABLE III
CONCENTRATION CHANGE OF SIMULATED GASES IN THE ABSENCE OF OXYGEN

	C_3H_8 <3510 ppm>	CO <4.02%>	NO{NO_2} <1215 ppm>
Before discharge	3362 (3331)	4.04 (4.19)	972 {32}
After discharge	1233 (1457)	3.97 (4.02)	492 {20}

< > shows a calculated concentration of C_3H_8, CO and NOx.

( ) shows a measurement concentration of C_3H_8 and CO with CO/HC analyzer.

{ } shows a concentration of NO_2.

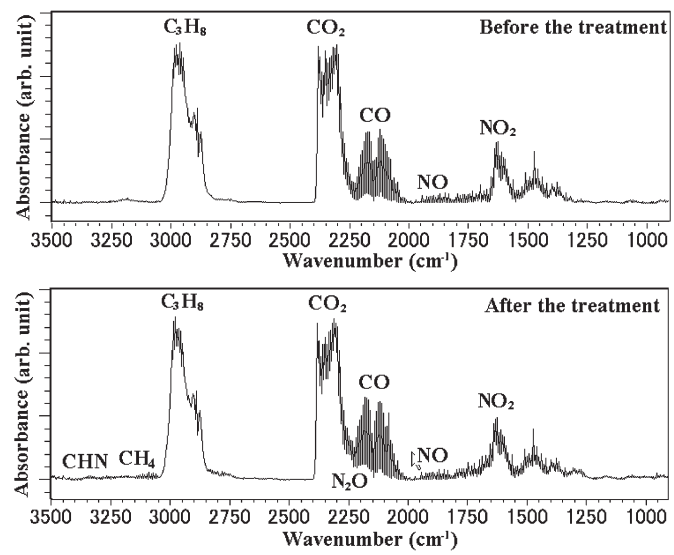

Fig. 12. By-product analysis obtained by FTIR in the existence of O_2. Gas composition: 3.82% CO, 3335-ppm C_3H_8, 1154-ppm NO, 11.42% CO_2, 5% O_2, and N_2 balance. Discharge voltage: 1.3 kV. Discharge gap: 10 μm. Gas flow rate: 0.5 L/min.

As shown in Fig. 11 and Table III, HCN, CH_4, and N_2O are confirmed as by-products, and C_3H_8, CO, and NO are decomposed by a microplasma after the discharge. According to Table III, the amount of C_3H_8 decreases in the absence of O_2, resulting in the formation of HCN and CH_4.

Fig. 12 shows the spectra of by-product analysis obtained by FTIR with oxygen concentration of 5%.

The experimental conditions of Fig. 11 are at a discharge voltage of 1.3 kV and a discharge gap of 10 μm. The gas composition of the simulated gas is adjusted to 3.82% CO, 3335-ppm C_3H_8, 1154-ppm NO, 11.42% CO_2, 5% O_2, and N_2 balance. The upper figure shows the spectrum of before the treatment with microplasma, and the lower figure shows that of after the treatment.

Table IV shows the changes of the concentration of simulated gas by a microplasma with oxygen concentration of 5%. These are estimated from the FTIR spectra and by using a NO_x analyzer and a CO/HC analyzer.

As shown in Fig. 12 and Table IV, HCN, CH_4, CO, NO_2, and N_2O are generated as by-products, and C_3H_8 and NO are decomposed by a microplasma after the discharge. According

TABLE IV
CONCENTRATION CHANGE OF SIMULATED GASES WITH 5% OXYGEN

	C_3H_8 <3335 ppm>	CO <3.82%>	NO {NO_2} <1154 ppm>
Before discharge	3198 (3281)	3.95 (4.1)	940 {145}
after discharge	2826 (2974)	4.62 (4.79)	873 {313}

< > shows a calculated concentration of C_3H_8, CO and NOx.

( ) shows a measurement concentration of C_3H_8 and CO with CO/HC analyzer.

{ } shows a concentration of NO_2.

to Table IV, the amount of C_3H_8 decreases in the presence of O_2, with C reacting with O, and it results in the formation of CO and also of HCN and CH_4.

C. Energy Efficiency for Gas Treatment

The specific input energy (SIE) is defined as the total discharge power dissipated per unit volume of the gas [23]

$$\text{SIE [J/L]} = \text{Electrical Input Power [J/s]} / \text{Gas Flow Rate [L/s]}. \quad (10)$$

Fig. 7 shows the characteristics of the discharge power and the discharge voltage of microplasma in air. For a discharge gap of 10 μm and a discharge voltage of 1.2 kV, a corresponding electrical input power of 7 W was measured. At a gas flow rate of 5 L/min, according to (10)

$$\text{SIE}_{(1.2\text{ kV and 10-}\mu\text{m gap})} = 7/0.0833 = 84 \text{ J/L}. \quad (11)$$

The measurements of the discharge power and discharge voltage shown in Fig. 7 were performed for one pair of electrodes. The measured power contains also the losses in the power-supply circuit. Two pairs of electrodes were used in order to measure the discharge power. At a discharge voltage of 1.2 kV and a discharge gap of 10 μm, a discharge power of 9.5 W was measured. By subtracting the value of the discharge power shown in Fig. 7 for the discharge voltage of 1.2 kV, the 2.5-W value of the discharge power for one pair of electrodes is obtained. Thus, according to (10), the SIE for one pair of electrodes is

$$\text{SIE}_{(1.2\text{ kV and 10-}\mu\text{m gap})} = 2.5/0.0833 = 30 \text{ J/L}. \quad (12)$$

According to Fig. 8, for the gas composition of 100-ppm NO and N_2 balance, the NO removal concentration at the discharge voltage of 1.2 kV was 28 ppm. The energy efficiency at this discharge voltage was 4.5 g (NO)/kW · h. Although the energy efficiency of the microplasma reactor is lower than that of the conventional plasma reactor [24], [25], due to the small sizes of the reactor and power supplies, microplasma is a technology that can be applied at mobile sources such as small automobiles and motorcycles.

VI. CONCLUSION

We have investigated treatment and removal of simulated gas by a microplasma. Removal of NO_x and HC by a microplasma is considered to be effective. The following are the conclusions drawn from a series of experiments.

1) Microplasma is generated around 1 kV at a discharge gap of 10 μm.
2) When the simulated gas, including NO, O_2, and N_2, is treated by a microplasma, the value of NO_x removal is maximum at a certain discharge voltage.
3) When the simulated gas, including NO, C_3H_8, O_2, and N_2, is treated by a microplasma, the concentration of NO_x increases, and the oxidation of NO to NO_2 decreases. This phenomenon could be concerned with C_3H_8.
4) The oxygen and nitrogen atomic species generated by a microplasma could have oxidized NO to NO_2 and decomposed NO and C_3H_8. However, on simulated gas composition, CHN, CH_4, N_2O, and CO are confirmed as by-products.

REFERENCES

[1] S. Yagi and M. Tanaka, "Mechanism of ozone generation in air-fed ozonisers," *J. Phys. D, Appl. Phys.*, vol. 12, no. 9, pp. 1509–1520, Sep. 1979.

[2] J. Kitayama and M. Kuzumoto, "Theoretical and experimental study on ozone generation characteristics of an oxygen-fed ozone generator in silent discharge," *J. Phys. D, Appl. Phys.*, vol. 30, no. 17, pp. 2453–2461, Sep. 1997.

[3] J. Kitayama and M. Kuzumoto, "Analysis of ozone generation from air in silent discharge," *J. Phys. D, Appl. Phys.*, vol. 32, no. 23, pp. 3032–3040, Dec. 1999.

[4] D. Braun, U. Küchler, and G. Pietsch, "Microdischarges in air-fed ozonizers," *J. Phys. D, Appl. Phys.*, vol. 24, no. 4, pp. 564–572, Apr. 1991.

[5] B. M. Penetrante, M. C. Hsiao, B. T. Merritt, G. E. Vogtlin, P. H. Wallman, A. Kuthi, C. P. Burkhart, and J. R. Bayless, "Electron-impact dissociation of molecular nitrogen in atmospheric-pressure nonthermal plasma reactors," *Appl. Phys. Lett.*, vol. 67, no. 21, pp. 3096–3098, Nov. 1995.

[6] N. Goto and A. Kudo, "C_6H_6 decomposition using barrier discharge," *IEEJ Trans. FM*, vol. 126, no. 5, pp. 321–327, 2006.

[7] K. Shimizu and T. Oda, "DeNO_x process in flue gas combined with nonthermal plasma and catalyst," *IEEE Trans. Ind. Appl.*, vol. 35, no. 6, pp. 1311–1317, Nov./Dec. 1999.

[8] C. R. McLarnon and B. M. Penetrante, "Effect of gas composition on the NO_x conversion chemistry in a plasma," *SAE Trans.*, vol. 107, no. 4, pp. 886–897, 1998.

[9] L. A. Rosocha, G. K. Anderson, L. A. Bechtold, J. J.Coogan, H. G. Heck, M. Kang, W. H. McCulla, R. A. Tennant, and P. J. Wantuck, "Treatment of hazardous organic wastes using silent discharge plasmas," in *Proc. NATO Adv. Research Workshop Non-Thermal Plasma Tech. Pollution Control*, 1993, pp. 281–308.

[10] N. Hudo, H. Kurimoto, S. Kudo, and Y. Watanabe, "Decomposition of Benzene by barrier discharge inN_2 at low concentration of O_2," *IEEJ Trans. FM*, vol. 123, no. 9, pp. 900–905, 2003.

[11] Y. Yoshioka, "Application, and mutual comparison methods of exhaust gas treatment technology by various non-thermal plasma," *Trans. Inst. Elect. Eng. Jpn.*, vol. 122-A, no. 7, pp. 676–682, 2002.

[12] N. Goto, S. Kudou, and H. Motoyama, "Scaling relation for NO reduction by barrier discharge," *Trans. IEE Jpn.*, vol. 118-A, no. 7/8, pp. 888–894, 1998.

[13] B. M. Penetrante, M. C. Hsiao, B. T. Merritt, G. E. Vogtlin, W. M. Neiger, O. Wolf, T. Hammer, and S. Broer, "Pulsed corona and dielectric-barrier discharge processing of NO in N_2," *Appl. Phys. Lett.*, vol. 68, no. 26, pp. 3719–3722, Jun. 24, 1996.

[14] S. A. Nair, K. Yan, A. J. M. Pemen, E. J. M. van Heesch, K. J. Ptasinski, and A. A. H. Drinkenburg, "Tar removal from biomass derived fuel gas by pulsed corona discharge: A chemical kinetic study," *Ind. Eng. Chem. Res.*, vol. 43, no. 7, pp. 1649–1658, 2004.

[15] G. Dinelli, L. Civitano, and M. Rea, "Industrial experiments on pulse corona simultaneous removal of NO_x and SO_2 from flue gas," *IEEE Trans. Ind. Appl.*, vol. 26, no. 3, pp. 535–541, May/Jun. 1990.

[16] K. Tachibana, "Properties of microplasmas and their unique physics," *Trans. Inst. Elect. Eng. Jpn.*, vol. 1-S6-6, pp. 19–22, 2006.

[17] K. Shimizu, T. Sugiyama, N. L. S. Manisha, and M. Kanamori, "Application of micro discharge for air purification," *IEEJ Trans. PE*, vol. 127, no. 12, pp. 1269–1274, 2007.
[18] K. Shimizu, T. Sugiyama, and L. S. Manisha Nishamani, "Study of air pollution control by using micro plasma," in *Proc. ESA/IEEE-IAS/IEJ/SFE Joint Conf. Electrostat.*, 2006, vol. 2, pp. 873–882.
[19] R. Atkinson, D. L. Baulch, R. A. Cox, J. N. Crowley, R. F. Hampson, R. G. Hynes, M. E. Jenkin, M. J. Rossi, and J. Troe, "Evaluated kinetic and photochemical data for atmospheric chemistry: Part 1—gas phase reaction of O_x, HO_x, NO_x and SO_x species," *Atmos. Chem. Phys. Discuss.*, vol. 3, pp. 6179–6699, 2003.
[20] A. Mizuno, K. Shimizu, A. Chakrabarti, L. Dascalescu, and S. Furuta, "NO_x removal process using pulsed discharge plasma," *IEEE Trans. Ind. Appl.*, vol. 31, no. 5, pp. 957–963, Sep./Oct. 1995.
[21] K. Okazaki, T. Kishida, K. Ogawa, and T. Nozaki, "Direct conversion from methane to methanol for high efficiency energy system with energy regeneration," *Energy Convers. Manag.*, vol. 43, no. 9–12, pp. 1459–1468, 2002.
[22] S. Kado, Y. Sekine, K. Urasaki, K. Okazaki, and T. Nozaki, "High performance methane conversion into valuable products with spark discharge at room temperature," in *Proc. 7th Nat. Gas Convers., Stud. Surf. Sci. Catalyst*, 2004, vol. 147, pp. 577–582.
[23] S. Sato, M. Kimura, T. Aki, I. Koyamoto, K. Takashima, S. Katsura, and A. Mizuno, "Removal of diesel particles using an electrostatic precipitator with a barrier discharge electrode as a dust pocket," in *Proc. ESA/IEJ/IEEE-IAS/SFE Joint Conf. Electrostat.*, 2006, pp. 754–761.
[24] H. H. Kim, G. Prieto, K. Takashima, S. Katsura, and A. Mizuno, "Performance evaluation of discharge plasma process for gaseous pollutant removal," *J. Electrostat.*, vol. 55, no. 1, pp. 25–41, May 2002.
[25] T. Shoyama and Y. Yoshioka, "Theoretical study of methods for improving the energy efficiency of NO_x removal from diesel exhaust gases by silent discharge," *Elect. Eng. Jpn.*, vol. 161, no. 3, pp. 1–9, Jul. 2007.

Kazuo Shimizu (S'93–M'00) was born in Hamamatsu, Japan, in 1969. He received the B.S., M.S., and Ph.D. degrees in electrical engineering from Toyohashi University of Technology, Toyohashi, Japan, in 1991, 1993, and 1996, respectively.

From April 1996 to 2002, he was with The University of Tokyo, Tokyo, Japan, as an Assistant Professor with in Graduate School of Frontier Sciences. During 2002–2005, he was Secretary for Policy and a Member of the House of Representatives (formerly Parliamentary Secretary for Land, Infrastructure and Transport). He has been an Associate Professor with the Innovation and Joint Research Center, Shizuoka University, Hamamatsu, Japan, since 2005. His current interests include the physics of microplasma and its application to environmental protection.

Dr. Shimizu is a member of the Industry Applications Society of the Institute of Electrical Engineers of Japan and the Institute of Electrostatics Japan.

Takeki Sugiyama was born in Shizuoka, Japan, in 1983. He received the B.S. and M.S. degrees from Shizuoka University, Hamamatsu, Japan, in 2006 and 2008, respectively.

He is currently with Shizuoka Gas Company, Ltd., Shizuoka, Japan.

Manisha Nishamani L. S. was born in Colombo, Sri Lanka, on February 25, 1979. She received the B.S. degree in electrical and electronic engineering from Shizuoka University, Hamamatsu, Japan, in 2006. She is currently working toward the M.S. degree at the Royal Institute of Technology (KTH), Stockholm, Sweden.

She has been part of a research team that examines the application of nonthermal microplasmas for indoor-air purification and has wide research background regarding the reduction of indoor-air pollutants such as formaldehyde and NO_x with low energy consumption.

Masaki Kanamori was born in Yokosuka, Japan, in 1984. He received the B.S. and M.S. degrees from the Innovation and Joint Research Center, Shizuoka University, Hamamatsu, Japan, in 2007 and 2009, respectively.

He is currently with the Toshiba Carrier Corporation, Tokyo, Japan.